J Nanopart Res (2011) 13:6717–6724
DOI 10.1007/s11051-011-0578-6

RESEARCH PAPER

A wet chemical preparation of transparent conducting thin films of Al-doped ZnO nanoparticles

Konstantin Tarasov · Olivier Raccurt

Received: 18 December 2010 / Accepted: 11 September 2011 / Published online: 22 September 2011

Abstract A wet chemical deposition method for preparing transparent conductive thin films on the base of Al-doped ZnO (AZO) nanoparticles has been demonstrated. AZO nanoparticles with a size of 7 nm have been synthesised by a simple precipitation method in refluxed conditions in ethanol using zinc acetate and Al-isopropylate. The presence of Al in ZnO was revealed by the EDX elemental analysis (1.8 at.%) and UV–Vis spectroscopy (a blue shift due to Burstein–Moss effect). The obtained colloid solution with the AZO nanoparticles was used for preparing by spin-coating thin films on glass substrates. The film demonstrated excellent homogeneity and transparency ($T > 90\%$) in the visible spectrum after heating at 400 °C. Its resistivity turned to be excessively high ($\rho = 2.6\ \Omega$ cm) that we ascribe to a poor charge percolation due to a high film porosity revealed by SEM observations. To improve the percolation via reducing the porosity, a sol–gel solution was deposited "layer-by-layer" in alternation with layers derived from the AZO colloid followed by heating. As it was shown by optical spectroscopy measurements, the density of thus prepared film was increased more than twice leading to a significant decrease in resistivity to $1.3 \times 10^{-2}\ \Omega$ cm.

Keywords AZO nanoparticles · ZnO · Wet chemical deposition · Transparent conducting oxide · Solar cells

K. Tarasov · O. Raccurt (✉)
Laboratoire de nano-Chimie et de Sécurité des Nano-Matériaux, Département de Technologies des Nano-Matériaux, LITEN, CEA Grenoble, 17 rue des Martyrs, 38054 Grenoble Cedex 9, France
e-mail: olivier.raccurt@cea.fr

Introduction

ZnO is a low cost oxide with inherent *n*-type conductivity and is considered today as the most suitable transparent conducting oxide (TCO) to replace expensive indium–tin oxide in solar cells. ZnO attracts also much interest due to increased demands in various fields such as the production of LED, anti-UV and low-emission coatings, photoluminescent and sensor materials, photocatalysis, etc (Özgür et al. 2005; Klingshirn 2007; Schmidt-Mende and MacManus-Driscoll 2007; Weintraub et al. 2010).

Electro-conducting properties can be significantly improved if ZnO is doped with an element of the group III such as Al, In, Ga, etc. (Schmidt-Mende and MacManus-Driscoll 2007). Among them, aluminium is the most appropriate due to its low cost and small ionic radius. In literature, ZnO doped with Al^{3+} ions is normally abbreviated as AZO. The following quasi-chemical equation expressed in Kröger–Vink notations shows interrelation between the electron concentration and doping in ZnO:

$$n\mathrm{Zn_{Zn}}^{x} + n\mathrm{O_O}^{x} \xrightarrow{+\mathrm{Al_2O_3}} (n-2)\mathrm{Zn_{Zn}}^{x} + 2\mathrm{Al_{Zn}}^{\bullet} + (2+n)\mathrm{O_O}^{x} + 1/2\,\mathrm{O_2} \uparrow + 2\mathrm{e}' \quad (1)$$

For example, a partial replacement of Zn^{2+} by Al^{3+} in the ZnO structure ($Zn_{1-x}Al_xO_{1+x/2}$) allows increasing the electron concentration from about 10^{16} to 10^{21} cm^{-3} (Özgür et al. 2005; Minami 2005).

ZnO-based thin films can be prepared by various techniques: magnetron sputtering, pulsed laser deposition, CVD and solution (also called "wet") deposition (Exarhos and Zhou 2007). First three techniques are the most widely used methods permitting to prepare TCO films endowed with a good conductivity ($\rho < 10^{-3}$ Ω cm) and a high transparency ($T \geq 85\%$). However, the utilisation of these methods on industrial scale is limited by their complexity and high cost. The wet deposition methods, comprising spin-coating, dip-coating and spray techniques, are considered to be less expensive and are especially promising for fabricating large-area films (Aegerter et al. 2004).

The vast majority of the reports in literature regarding the wet methods for preparing AZO films deal with depositions from sol–gel solutions containing high concentrations of organic salts of zinc and a doping element (Ohyama 1998; Schuler and Aegerter 1999; Nasr et al. 2010). Oxide clusters appearing in sol–gel solutions are normally deposited together with the supernatant solution without preceding separation or washing, hence after each deposition a careful thermal treatment is needed to remove residual organic species. A typical preparation procedure of a film with a thickness of about 0.3–1 μm requires numerous repeated *deposition–calcination* cycles (Schuler and Aegerter 1999; Shinde et al. 2008) that represents a significant drawback of this method. An alternative approach involves a deposition using concentrated colloids with crystalline nanoparticles (Goebbert 1999; Lu et al. 2011). Such colloids give rise to thicker coatings, contain less organic species and, as a result, allow decreasing the cost of the overall preparation procedure. This approach has been demonstrated for preparing conducting films based on Sn-doped In_2O_3 and Sb-doped SnO_2 with resistivities close to those obtained by conventional methods (Goebbert 1999; Ederth et al. 2003; Aegerter and Al-Dahoudi 2006). Unfortunately, this approach has been scarcely studied in relation to ZnO thin films. Apparently, one of the reasons is the difficulty to synthesise stable colloids of crystalline nanoparticles of ZnO, pure in phase composition, uniform in shape and size and doped sufficiently with a trivalent cation required for obtaining films with good electroconducting properties and transparency. Van den Rul et al. (2006) explored different chemical pathways to ZnO colloids including hydrothermal, microemulsion, controlled double-jet precipitation and aqueous sol–gel methods. The authors claimed that only the latter method was suitable for preparing doped nanoparticles. Applying this sol–gel method and using ZnO powder, ethylenediamine as a base and Al-citrate as a doping agent, after 20 depositions–calcinations cycles and heating at 500 °C, the authors obtained a thin film with a resistivity of about 5×10^{-3} Ω cm and a transparency of about 90%. Unfortunately, the preparation procedure of the colloid and the characterisation of the obtained films were not presented in detail. In the work of Lu et al. (2011), a well crystallised Al-doped ZnO (AZO) nanoparticles with an average size of 40 nm were synthesised by a solvothermal method. The product powders heated in hydrogen at 700 °C and compressed into a coin shape pellets demonstrated, however, a rather high resistivity of 2.2×10^{1} Ω cm. Interesting results were achieved by Gomez-Pozos et al. (2007) for AZO films with a thickness of 0.6 μm prepared by a chemical spray technique. After a vacuum-thermal treatment at 400 °C, a film deposited at 475 °C and containing 3 at% of Al showed the minimum resistivity as low as 4.3×10^{-3} Ω cm with an optical transparency between 85 and 90%.

We dedicated this work to investigating TCO films deposited using colloids of AZO nanoparticles prepared via a modified chemical precipitation method. The obtained nanoparticles and thin films were characterized using X-ray diffraction, electron microscopy, UV–Vis spectroscopy and electric resistivity measurements.

Experimental

Syntheses

The synthesis procedure was close to that reported for preparing nanocrystals of undoped ZnO (Spanhel and Anderson 1991). Some modifications were introduced in the procedure to insure doping ZnO with Al. 0.225 g

of aluminium isopropylate $Al[(CH_3)_2CHO]_3$ and 10.98 g of zinc acetate dihydrate $Zn(CH_3COO)_2{\cdot}2H_2O$ were dissolved in 500 mL of ethanol. Then the resulted solution was refluxed at 85 °C until 200 mL of ethanol was evaporated. KOH was taken instead of LiOH to avoid a possible co-doping with Li^+. 4.21 g of KOH was added to the solution and dissolved using an ultrasonic bath to obtain a transparent solution. 3 mL of water were added drop-wise in the boiling solution under constant agitation using a magnetic stirrer. After adding water, the solution was tightly closed and agitated during 16 h at room temperature. The resulted AZO nanoparticles were separated from the supernatant solution by centrifugation, washed with ethanol thrice and redispersed in ethanol. To stabilize the obtained AZO colloid, diethanolamine (DEA) was added to ensure the molar ratio of Zn/DEA equal to 1.0.

A sol–gel solution contained 0.3 M zinc acetate and aluminium nitrate with an atomic ratio Al/(Al + Zn) = 2%. The salts were dissolved in 2-propanol and stabilized by DEA according to the procedure reported elsewhere (Schuler and Aegerter 1999).

Film deposition and annealing process

The films were prepared on square glass substrates Corning Eagle XG™ of sizes 1 in. × 1 in. The depositions were performed using a spin-coater with a rotation speed of 3000 rpm. After each 5 depositions from the AZO colloid, the resulted film was dried at 120 °C for 10 min and then heated in air at 400 °C for 15 min. For preparing a sample with alternating layers from two different precursor solutions, the heating was carried out at 120 °C for 15 min after a deposition from the AZO colloid and at 400 °C for 15 min after a deposition from the sol–gel solution. For all samples, heating at 400 °C for 30 min in a flow of hydrogenated nitrogen (4% H_2) was applied as the final treatment.

Characterisation

The size distribution of hydrodynamic diameters (d_h) of AZO colloids was determined using an Malvern Instrument of dynamic light scattering (DLS) "Zeta-Sizer Nano". The measurements were carried out at 25 °C. TEM characterisation and elemental analysis of the AZO particles were performed using a JEOL 2000FX microscope coupled with an EDX set-up. The samples were prepared by placing a drop of a diluted colloid on a copper grid and drying in air. The optic properties of colloids and films were characterised with the aid of a UV–Vis spectrometer Shimadzu-3100. The transmittance spectra of the films were recorded without subtracting the contribution of the substrate. The phase composition was characterised by a D8 Bruker diffractometer using Cu$K\alpha$ radiation. Crystal size was determined with the use of the Scherrer equation (West 1984). SEM images of the films were taken using a Hitachi 4000 microscope. The film resistivities were found by considering film thicknesses and surface resistances measured using a Loresta HP MCP-T4104 resistivity-meter equipped with a 4-point electrode.

Results and discussion

Preparation of colloids with AZO nanoparticles

The preparation of nanoparticles of undopped ZnO by means of the controlled hydrolysis of zinc acetate in refluxing conditions in ethanol allows obtaining especially small nanoparticles (Spanhel and Anderson 1991). For successful introduction of Al^{3+} ions into ZnO, an appropriate aluminium-containing precursor was needed. Several authors reported difficulties with homogeneous incorporation of aluminium cations into ZnO when aluminium inorganic salts were used (Strachowski 2007; Chakraborty et al. 2008; Nie et al. 2008). On the other hand, utilisation of organic precursors such as acetate (Kadam et al. 2008) or acetylacetonate (Thu and Maenosono 2010; Gomez-Pozos et al. 2007) allowed obtaining homogeneously doped AZO films. We used aluminium isopropylate, $Al[(CH_3)_2CHO]_3$, which is known as a convenient precursor for synthesis of fine alumina by hydrolytic decomposition (Grinberg et al. 2002). The concentration of Al^{3+} in the starting solution was 2.5 at.% in respect to the sum of molar concentrations of zinc and aluminium. According to the EDX chemical analysis, the aluminium content in the washed final product was slightly lower (1.8 at.%). The dispersion of the obtained solid in ethanol in the presence of DEA gave rise to a slightly opalescent colloid. The presence of the stabilizing agent DEA was needed for arresting further crystal growth and aggregation.

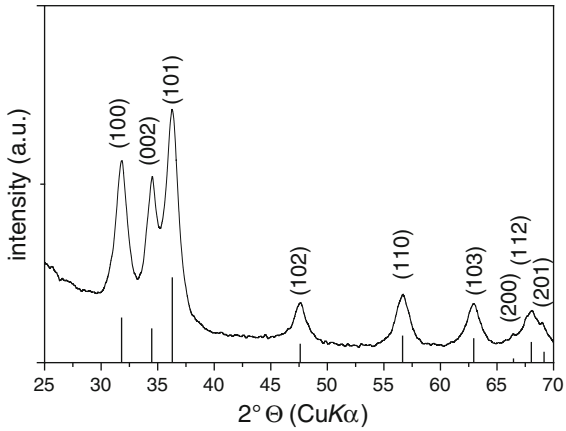

Fig. 1 XRD pattern of synthesized AZO nanoparticles. *Straight lines* represent a reference pattern of wurtzite ZnO (JCPDS card no. 36-1451)

The obtained particles separated from the supernatant solution, washed and dried in air, were characterised by XRD and TEM. It was found that the solid represents wurtzite, a polymorph of ZnO, and no aluminium-containing phases were detected (Fig. 1). The absence of individual phases enriched in aluminium was also confirmed by the probe EDX analysis which showed a homogeneous distribution of aluminium throughout the whole sample. The significant broadening of the XRD peaks indicates that ZnO occurs in a nanocrystalline or disordered state. The crystal size found using the Scherrer formula is in good agreement with the average particle size found by TEM (Table 1). TEM studies also revealed that the dried sample represent monodisperse particles consolidated in crosslinked aggregates with sizes between 20 and 80 nm (Fig. 2). In fact, these aggregates are formed already in the colloid rather than after drying the sample: the DLS measurement (Fig. 3) reveals in the colloid solution large scattering centres with a mean diameter of 52 nm that is close to the aggregate sizes observed by TEM.

Further characterisation of the obtained AZO colloid was performed using UV–Vis absorption spectroscopy. Figure 4 shows an absorption spectrum

Table 1 Particles sizes in the AZO colloid found by different methods

Sample	d_{XRD} (nm)	d_{TEM} (nm)	d_{UV-Vis} (nm)
AZO colloid	6.9	7.1	4.6

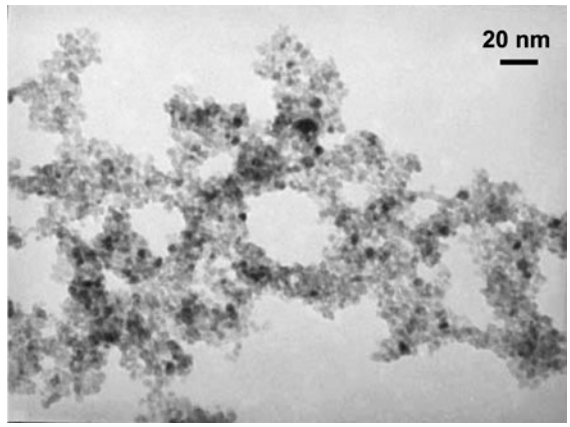

Fig. 2 TEM image of AZO nanoparticles

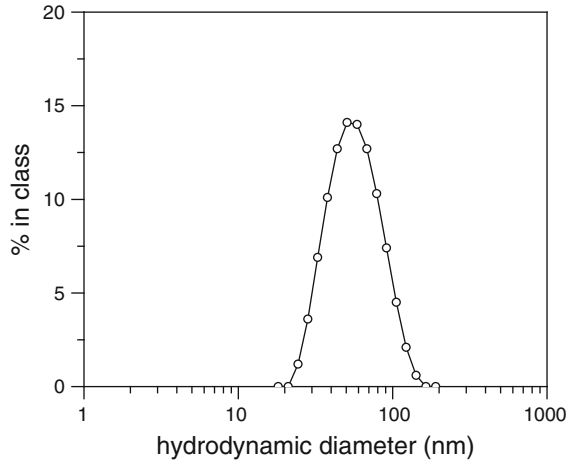

Fig. 3 Size-distribution obtained by DLS of colloid solution with AZO nanoparticles (diluted 1:100)

of the colloid where one can see a distinct shoulder at about 340 nm. Such a shoulder situated in the ultraviolet range of the spectrum is characteristic of the ZnO exciton band. For a direct band gap semiconductor such as ZnO, the energy between the valence and conduction bands, i.e. the band gap energy (E_g), can be found from the UV–Vis spectra near the absorption edge using the following equation (Pankove 1971):

$$\alpha = C\left(hv - E_g\right)^{1/2} \tag{2}$$

where α is the absorption coefficient, C is a constant and hv is the photon energy. The E_g value was obtained by extrapolating the linear segment of the plot $\alpha^2 = f(hv)$ to $\alpha = 0$ as shown in the inset in Fig. 4.

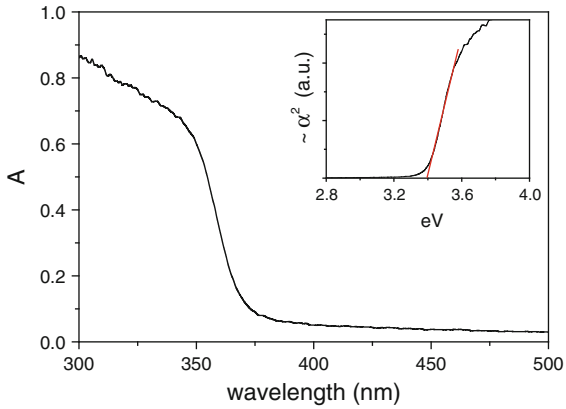

Fig. 4 Absorption spectrum of colloid solution with AZO nanoparticles (diluted 1:100). In the inset: a plot showing the method of determining E_g

Compared to the band gap energy 3.3 eV reported for bulk ZnO at room temperature (Srikant and Clarke 1998), the obtained energy $E_g = 3.40 \pm 0.06$ eV is notably higher. Such an increase in E_g is characteristic of the quantum-confinement effect in ZnO (Yoffe 2002). This effect manifests itself in absorption spectra as a blue-shift of the exciton band in such a way that the smaller the nanoparticles the stronger the blue-shift.

With the aid of the optical absorption spectroscopy one can alternatively find the particle size using the inflection point of the exciton absorption band ($\lambda_{1/2}$) and an empirical formula determined for ZnO particles in the size range from 2 to 7 nm (Meulenkamp 1998). The value $\lambda_{1/2} = 360.3$ nm calculated by differentiation gives a particle size of 4.6 nm. This is notably lower than the size found by TEM and XRD (Table 1). We ascribe this inconsistency to an additional blue-shift due to introduction of Al^{3+} ions into ZnO. The Al^{3+}-substituting for Zn^{2+} causes an increase in the electron concentration as shown in Eq. 1. This effect, known in the literature as the effect of Burstein–Moss, is established as $\Delta E_g \sim n^{2/3}$ (Basu 1997). Therefore, the observed additional shift of the exciton band may provide another evidence of the incorporation of Al^{3+} in the bulk of ZnO (Kadam et al. 2008).

Characterisation of AZO films

Figure 5 shows SEM images of an AZO film prepared by spin-coating followed by heating at 400 °C. As seen from the presented images, the film was evenly deposited on the substrate and is composed of grains with sizes of about 10 nm. The film has a porous morphology due to evaporation of the solvent and DEA molecules upon drying and heating.

The XRD pattern of the film (Fig. 6) shows wide peaks attributable to wurtzite. The relative intensities of the first three peaks (reflections (100), (002) and (110)) are in agreement with the literature data for randomly orientated ZnO crystals. This implies that there is no or little preferred orientation of the AZO crystals on the substrate, in agreement with the SEM observations. The post-synthesis thermal treatment gave rise to a particle size growth: the crystal size, according to XRD measurements, became 9.7 nm.

The increase in the particle size leads to a "red-shift" of the exciton band absorption of ZnO as evidenced by a decrease in the band gap energy to 3.31 ± 0.02 eV. The spectrum recorded in the transmission mode and presented in Fig. 7 shows that the film has an excellent transparency being around 90% in the range of 400–900 nm. However, the film electrical

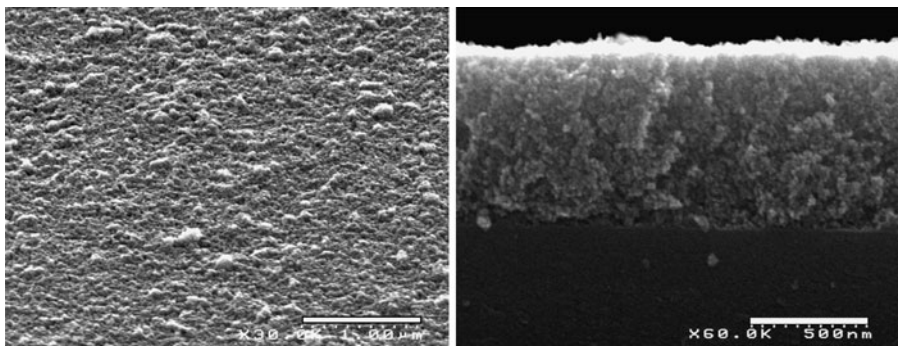

Fig. 5 SEM images of the surface (*left*, scaling bar 1 μm) and a cross-section (*right*, scaling bar 500 nm) of a film prepared from colloid solution with AZO nanoparticles

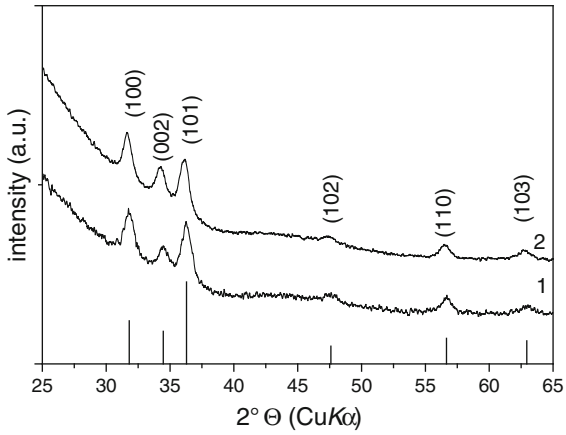

Fig. 6 XRD pattern of films deposited from colloid solution with AZO nanoparticles (1) and from the same solution deposited in alternation with a sol–gel solution (2). *Straight lines* represent a reference pattern of wurtzite ZnO (JCPDS card no. 36-1451)

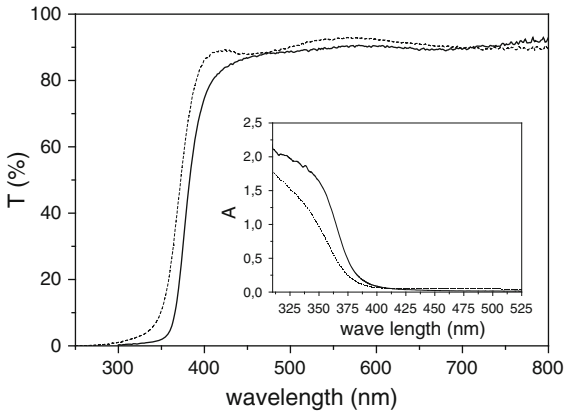

Fig. 7 Transmission spectra of films deposited from colloid solution with AZO nanoparticles (*full line*) and from the same solution deposited in alternation with a sol–gel solution (*dashed line*). In the *inset*: corresponding absorption spectra

resistivity was found to be rather high (2.6 Ω cm) that can be associated with a poor charge percolation due to a high film porosity (Ofir et al. 2008; Oosterhout et al. 2009).

To decrease film porosity, we used a sol–gel solution prepared by a standard procedure (Schuler and Aegerter 1999). The sol–gel solution containing zinc and aluminium ions in the proportion (Al/(Al + Zn) = 2 at%) was deposited by spin-coating in alternation with the AZO colloid solution "layer-by-layer". Such a "mixed" deposition allowed impregnating inter-particle voids appearing in the "colloid" layer by the sol–gel solution leading to an enhancement of the film compactness. An increase in film density was revealed by optical absorption measurements. In the region of the exciton band, the film absorption A conforms to the Beer–Lambert law:

$$A = \alpha L \tag{3}$$

where L is the film thickness and α is the absorption coefficient. Provided that the film thickness is known and applying Eq. 3, one can easily find the absorption coefficient. The values of α presented in Table 2 were found for absorption at around 360 nm that corresponds to the inflection point position in the exciton absorption curves. One can see that for the film prepared only from the colloidal solution with AZO nanoparticles α is nearly twice lower than that for the film prepared using alternating depositions from two types of solutions. Since the absorption coefficient is proportional to the concentration of the substance (or to the density of absorbers in the layer), one can deduce thus that the latter film is about twice denser as well. Such an increase in film density was accompanied by a significant decrease in resistivity to 1.3×10^{-2} Ω cm. It is worthy to note that such a "mixed" deposition does not worse good transparency of the film that remained about 90% in the visible range of the spectrum (Fig. 7). It is interesting that the exciton band absorption of the "mixed" film is slightly "blue"-shifted in comparison with the one of the film prepared using only the AZO colloid. This phenomenon can be due to an enhanced incorporation of aluminium ions into ZnO in the "mixed" film.

Conclusion

In this article, we have demonstrated that 7-nm particles of AZO (2 at%) can be prepared by precipitating in refluxed conditions using zinc acetate and Al-isopropylate as a doping agent. To avoid difficulties with homogeneous incorporation of aluminium cations into ZnO, we replaced the widely used doping agents such as aluminium nitrate, chloride or citrate by an organometallic compound, Al-isopropylate. The homogeneous incorporation of Al in ZnO was confirmed by EDX analysis as well as by UV–Vis spectroscopy revealing a blue shift due to Burstein–Moss effect.

Table 2 Crystal size, thickness, optical and electroconducting properties of the films prepared by different ways of deposition

Sample	d_{XRD} (nm)	Thickness L (nm)	ρ (Ω cm)	T (at 550 nm) (%)	α (cm^{-1})
AZO film from colloid solution	9.7	750	2.6	90	2.0×10^4
AZO film from colloid and sol–gel solutions	10.3	230	1.3×10^{-2}	92	4.3×10^4

The synthesized AZO particles, dispersed and stabilized in 2-propanol, were further deposited in the form of thin films using the spin-coating technique. As-deposited film was heated at 400 °C and demonstrated excellent transparency ($T > 90\%$) in the visible spectrum. Its resistivity, however, was relatively high ($\rho = 2.6\ \Omega$ cm) that was ascribed to a poor charge percolation owing to a high film porosity. To improve the percolation we used a sol–gel solution deposited "layer-by-layer" in alternation with layers derived from the AZO colloid. As it was shown by optical spectroscopy measurements, the density of thus prepared film was increased more than twice. As a result, the resistivity of the film was decreased to $1.3 \times 10^{-2}\ \Omega$ cm.

The obtained results show the difficulty in achieving an efficient charge percolation in films prepared by a wet chemical deposition of nanoparticles pointing out on the necessity of increasing the contact surface in the film. This goal can be achieved, as shown in our work, by alternating deposition of nanoparticles and sol–gel films. We admit that the wet chemical deposition method investigated in this study is potentially applicable for preparing coatings with large surfaces at relatively low costs. Although the electroconducting properties of the obtained films are quite modest, we expect to improve them by optimising the conditions of the post-synthesis thermal treatment in our future study.

Acknowledgements The authors thank Nathalie Scheer for her assistance in obtaining TEM images and the "Carnot Energie du Futur" for financial support.

References

Aegerter MA, Al-Dahoudi N (2006) Comparative study of transparent conductive In2O3:Sn (ITO) coatings made using a sol and a nanoparticle suspension. Thin Solid Films 502(1–2):193–197. doi:10.1016/j.tsf.2005.07.273

Aegerter MA, Puetz J, Gasparro G, Al-Dahoudi N (2004) Versatile wet deposition techniques for functional oxide coatings. Opt Mater 26:155–162

Basu PK (1997) Theory of optical processes in semiconductors: bulk and microstructures. Oxford University Press, New York

Chakraborty A, Mondal T, Bera SK, Sen SK, Ghosh R, Paul GK (2008) Effects of aluminum and indium incorporation on the structural and optical properties of ZnO thin films synthesized by spray pyrolysis technique. Mater Chem Phys 1:162–166. doi:10.1016/j.physletb.2003.10.071

Ederth J, Johnsson P, Niklasson GA, Hoel A, Hultaker A, Heszler P, Granqvist CG, Van Doom AR, Jongerius MJ, Burgard D (2003) Electrical and optical properties of thin films consisting of tin-doped indium oxide nanoparticles. Phys Rev B 68:155410. doi:10.1103/PhysRevB.68.155410

Exarhos GJ, Zhou XD (2007) Discovery-based design of transparent conducting oxide films. Thin Solid Films 515:7025–7052. doi:10.1016/j.tsf.2007.03.014

Goebbert C, Nonninger R, Aegerter MA, Schmidt H (1999) Wet chemical deposition of ATO and ITO coatings using crystalline nanoparticles redispersable in solutions. Thin Solid Films (1–2):79–84. doi:10.1016/S0040-6090(99)00209-6

Gomez-Pozos H, Maldonado A, de la L Olvera M (2007) Effect of the [Al/Zn] ratio in the starting solution and deposition temperature on the physical properties of sprayed ZnO:Al thin films. Mater Lett 7:1460–1464. doi:10.1016/j.matlet.2006.07.053

Grinberg EE, Saradzhev VV, Levin YI, Ryabenko EA (2002) Preparation of fine alumina powders by hydrolysis of aluminum isopropylate 2:245–247. doi:10.1023/A:1016108302641

Kadam P, Agashe C, Mahamuni S (2008) Al-doped ZnO nanocrystals. J Appl Phys 104:103501. doi:10.1063/1.3020527

Klingshirn C (2007) ZnO: material, physics and applications. Chem Phys Chem 8:782–803. doi:10.1002/cphc.200700002

Lu Z, Zhou J, Wang A, Wang N, Yang X (2011) Synthesis of aluminium-doped ZnO nanocrystals with controllable morphology and enhanced electrical conductivity. J Mater Chem 21:4161–4167

Meulenkamp EA (1998) Synthesis and growth of ZnO nanoparticles. J Phys Chem B 102:5566–5572

Minami T (2005) Transparent conducting oxide semiconductors for transparent electrodes. Semicond Sci Technol 20:S35–S44. doi:10.1088/0268-1242/20/4/004

Nasr B, Dasgupta S, Wang D, Mechau N, Kruk R, Hahn H (2010) Electrical resistivity of nanocrystalline Al-doped zinc oxide films as a function of Al content and the degree of its segregation at the grain boundaries. J Appl Phys 108:103721(1-6). doi:10.1063/1.3511346

Nie DP, Xue T, Zhang Y, Li XJ (2008) Synthesis and structure analysis of aluminium doped zinc oxide powders. Sci Chin Ser B: Chem 9:823–828

Ofir A, Dor S, Grinis L, Zaban A, Sittrich T, Bisquert J (2008) Porosity dependence of electron percolation in nanoporous TiO_2 layers. J Chem Phys 128:064703(1-9). doi:10.1063/1.2837807

Ohyama M, Kozuka H, Yoko T (1998) Sol-gel preparation of transparent and conductive aluminium-doped zinc oxide films with highly prepferential crystal orientation. J Am Ceram Soc 6:1622–1632. doi:10.1111/j.1151-2916.1998.tb02524.x

Oosterhout SD, Wienk MM, van Bavel SS, Thiedmann R, Koster LJA, Gilot J, Loos J, Scmidt V, Janssen RAJ (2009) Nat Mater 8:818–824. doi:10.1038/NMAT2533

Özgür Ü, Alivov YI, Liu C, Teke A, Reshchikov MA, Doğan S, Avrutin V, Cho S-J, Morkoç H (2005) A comprehensive review of ZnO materials and devices. J Appl Phys 98:041301(1-103). doi:10.1063/1.1992666

Pankove PI (1971) Optical processes in semiconductors. Dover, New York, p 412

Schmidt-Mende L, MacManus-Driscoll JL (2007) ZnO—nanostructures, defects, and devices. Mater Today 5:40–48. doi:10.1016/S1369-7021(07)70078-0

Schuler T, Aegerter MA (1999) Optical, electrical and structural properties of sol gel ZnO:Al coatings. Thin Solid Films 351:125–131

Shinde SS, Shinde PS, Pawar SM, Moholkar AV, Bhosale CH, Rajpure KY (2008) Physical properties of transparent and conducting sprayed fluorine doped zinc oxide thin films. Solid State Sci 10:1209–1214

Spanhel L, Anderson MA (1991) Semiconductor clusters in the sol–gel process: quantized aggregation, gelation, and crystal growth in concentrated ZnO colloids. J Am Chem Soc 113:2826–2833

Srikant V, Clarke DR (1998) On the optical band gap of zinc oxide. J Appl Phys 83(10):5447–5451. doi:10.10063/1.367375

Strachowski T (2007) Morphology and luminescence properties of zinc oxide nanopowders doped with aluminum ions obtained by hydrothermal and vapor condensation methods. J Appl Phys 102:073513(1-9). doi:10.1063/1.2786707

Thu T, Maenosono S (2010) Synthesis of high quality Al-doped ZnO nanoink. J Appl Phys 107:014308(1-6). doi:10.1063/1.3273501

Van den Rul H, Mondelaers D, Van Bael MK, Mullens J (2006) Water-based wet chemical synthesis of (doped) ZnO nanostructures. J Sol–Gel Sci Technol 39:41–47. doi:10.1007/s10971-006-6322-5

Weintraub B, Zhou Z, Li Y, Deng Y (2010) Solution synthesis of one-dimensional ZnO nanomaterials and their application. Nanoscale 2:1573–1587. doi:10.1039/C0NR00047G

West AR (1984) Solid state chemistry and its application. Wiley, Chichester

Yoffe AD (2002) Low-dimensional systems: quantum size effects and electronic properties of semiconductor microcrystallites (zero-dimensional systems) and some quasi-two-dimensional systems. Adv Phys 51(2):799–890. doi:10.1080/00018730110117451